Effect of friction stir processing on mechanical and microstructural properties of AM60B Magnesium alloy

P. CAVALIERE*, P. P. DE MARCO
INFM-Dept. of "Ingegneria dell'Innovazione", Engineering Faculty, University of Lecce, Via per Arnesano, 73100 Lecce, Italy
E-mail: pasquale.cavaliere@unile.it

Published online: 12 April 2006

Some AM60B magnesium alloys sheets produced by High Pressure die Casting were Friction Stir Processed and the mechanical and microstructural features are presented in the present study. The mechanical properties of the FSP material were analyzed in longitudinal direction respect to the processing one and compared with those of the base material. Tensile tests were performed at room and high temperature and different strain rates in the nugget zone, in order to analyse the superplastic properties of the recrystallized material and to observe the differences respect to the base material after the strong grain refinement effect due to the Friction Stir Process. The high temperature behaviour of the material was studied, in longitudinal direction, by means of tensile tests in the temperature and strain rate ranges of 175–250°C and 10^{-2}–10^{-4} s^{-1} respectively.

1. Introduction

Magnesium alloys components are very attractive for industrial applications in the transportation field because of their low density and the excellent room temperature strength and rigidity [1–3]. However, the use of magnesium alloys has been strongly limited because of their poor formability at near room temperature as a consequence of h.c.p. lattice. Many results have been published on the physical and mechanical properties of AM60 magnesium alloy [4, 5]. Many researchers demonstrated the existence of superplastic behaviour of a lot of Magnesium alloys and composites [3–7]. It is clear that it is possible to achieve superplasticity at high strain rates, in conventional alloys, by making a strong reduction in grain size; this can be obtained by using a process such as Equa-Channel-Angular pressing, High Pressure Torsion or Friction Stir Processing in which the samples are subjected to a severe plastic deformation leading to a strong grain refinement [8, 9].

In the Friction Stir Processing, a rotating tool, with a specially designed rotating probe, travels down the surfaces of metal plates, and produces a highly plastically deformed zone through the associated stirring action. The localized thermo-mechanical affected zone is produced by friction between the tool shoulder and the plate top surface, as well as plastic deformation of the material in contact with the tool [10]. The probe is typically slightly shorter than the thickness of the work piece and its diameter is typically the thickness of the work piece [11]. The FSP is a solid state process and therefore solidification structure is absent and the problem related to the presence of brittle intrer-dendritic and eutectic phases is eliminated [12].

The stirred zone consists of a weld nugget, thermo-mechanically affected zone and a heat affected zone. The process results in the obtaining of a very fine and equiaxed grain structure in the weld nugget obtained through a continuous dynamical recrystallization process causing a higher mechanical strength and ductility, the strong grain refinement produced by the process lead the microstructure to the fine dimensions proper of the possibility to exhibit superplastic properties. [13–15], recently interesting results on multi-step FSP, performed on AZ91D alloy, have been presented, showing the strong improving in formability properties due to the stirring action [16].

The aim of the present work is the study of the effect of Friction Stir Processing on the mechanical properties of HPDC AM60B sheets, and in particular the material behaviour in superplastic regime.

*Author to whom all correspondence should be addressed.
0022-2461
DOI: 10.1007/s10853-005-5601-9

TABLE I Chemical composition of the studied alloy (wt%)

	Mg (%)	Al (%)	Mn (%)	Si (%)	Cu (%)	Zn (%)	Fe (%)	Ni (%)	Be
AM60B	bal	5,97	0,30	0,012	0,0013	0.001	0.0008	0.0009	14.6 ppm

2. Experimental procedure

The AM60B magnesium alloy was supplied by Norsk Hydro Ltd. (Norway) in the high pressure die casting (HPDC) state into the form of cylindrical boxes measuring 2.5 mm thickness; the composition of the alloy is reported in Table I. From the boxes, some sheets were cutted and Friction Stir Processed by employing a steel flat tool with rotating speed of 700 RPM and a travelling speed of 2.5 mm/s, the tool was rotated in the clockwise direction while the specimens, fixed at the backing plate, were moved. The nib was 2.5 mm in diameter and 2.4 mm long, and a 20 mm diameter shoulder was machined perpendicular to the axis of the tool; the tilt angle of the tool was 3°.

The Vickers hardness profile of the of the material was measured on a cross-section and perpendicular to the processing direction using a Vickers indenter with a 200 gf load for 15 s.

Tensile tests were performed in order to evaluate the mechanical properties of the material obtained by FSP at room temperature and at higher temperatures (175–250°C) and different strain rates (10^{-2}–10^{-4} s^{-1}) by employing specimens obtained by EDM from the nugget zone cut parallel to the processing direction, the gauge dimensions were 30 × 3 × 1.2 mm; before tests, the surfaces of the specimens were mechanically polished in order to eliminate all the possible surface defects effects. The tensile tests were carried out using a LLOYD Instruments LR5K testing machine equipped with a resistance furnace.

The strain rate sensitivity coefficient (m) of the material was calculated employing the following equation:

$$m = \left.\frac{\partial \log \sigma}{\partial \log \dot{\varepsilon}}\right|_{\varepsilon,T} \quad (1)$$

The m value was calculated by interpolating the data obtained by hot tensile tests at an equivalent strain of 1. The cubic interpolation was applied between σ and $\dot{\varepsilon}$ logarithmic values.

Surfaces were prepared by standard metallographic techniques and etched with acetic-picral etchant (10 ml acetic acid, 4.2 g picric acid, 10 ml water, and 70 ml ethanol) for microstructural observations. A scanning electron microscope equipped with field emission gun (JEOL-JSM 6500 F) was employed for the observation of the fracture surfaces of the specimens tested in tension in order to study the microscopic defects of the joints and the mechanisms involved during deformation in the FSP and the base material.

3. Results and discussion

The as received material (Fig. 1a) showed a classical cast structure characterized by floating crystals, formed as a consequence of the very fast cooling, embedded in the eutectic phase.

Light microscopy observations were widely performed on the transverse cross-sections of the specimens, the FSP AM60B HPDC magnesium alloy revealed the classical formation of the elliptical "onion" structure in the centre of the specimen; this is a structure characterized by fine and equiaxed recrystallized grains (Fig. 1b), the higher temperature and severe plastic deformation results in grains recrystallized with a strong different structure respect to the as-cast as received material, a statistical analysis on 200 grains lead to a measurement of a mean grain size of 4 microns with a standard deviation of 0.5.

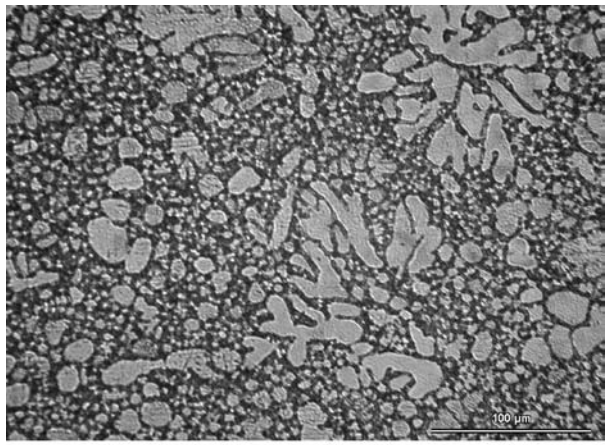

(a)

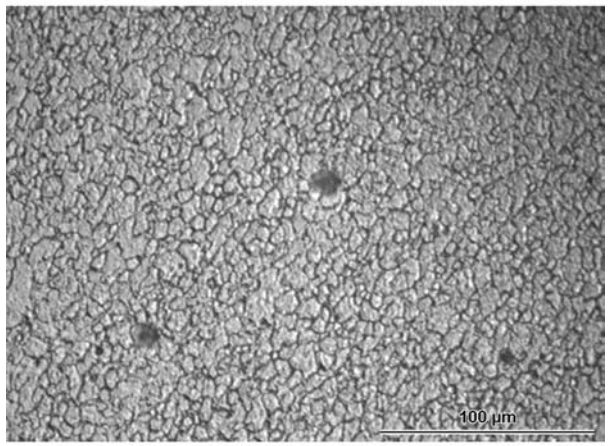

(b)

Figure 1 Optical microstructure of the as-received HPDC AM60B magnesium alloy (a) and of the strong grain refined structure consequent to the FSP (b).

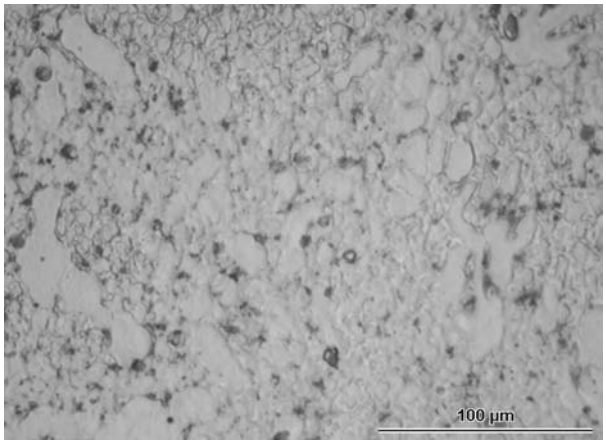

Figure 2 Optical microstructure of the Heat Affected Zone.

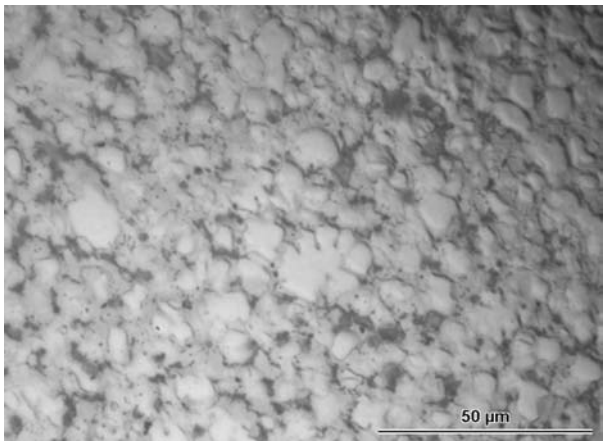

Figure 3 Optical microstructure of the Thermo Mechanically Affected Zone.

At a distance of 4 mm from the centre many of the prior grains and eutectic phase of the parent material start to appear (Fig. 2). This region corresponds to the heat affected zone as the hardness is low compared to the base material. The hardness drops here because the precipitates are coarsened. In the region adjacent to the nugget, i.e. TMAZ no recrystallization is observed because the temperature derived from the friction stir processing is not high enough and the deformation is not so severe to cause recrystallization (Fig. 3).

Such behaviour is confirmed by the microhardness profile (Fig. 4) along the FSP roads, the micro hardness reaches a value of 78 Hv in the centre of the weld and after increasing in both sides it starts to decrease after 2 mm from the centre until reaching a plateau corresponding to the hardness values of the parent material; in the centre the hardness is higher for the effect of casting defects closure and homogenisation.

The hardness of the joint reaches lower values in the HAZ respect to the parent material, this is a classical behaviour in the FSP light alloys, in the HAZ and TMAZ, in fact, the competing mechanisms of work hardening and over-ageing produce a strength decreasing respect to the stirred zone and the base material.

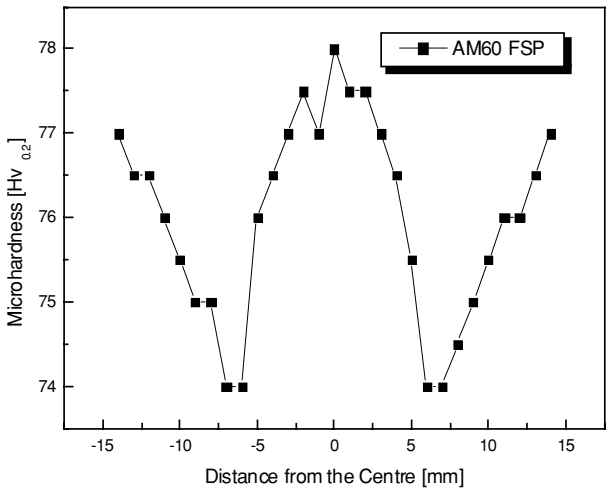

Figure 4 Microhardness profile of the central line of the stirred zone.

The tensile behaviour of the studied material in the as received and FSP conditions is plotted in Fig. 5. The FSP produces a strong increase in mechanical strength respect to the base material with also an increase in the elongation to failure; such behaviour was due to the disappearance of voids, caused by the HPDC, produced by the stirring action.

In Fig. 6 the fracture surfaces of the base material are shown, the material exhibits a ductile behaviour demonstrated by the presence of fine dimples but, the surfaces showed the presence of very large voids produced during the casting process. The increase in tensile strength after FSP is due, principally, to the voids closure produced by the stirring action (Fig. 7).

The True stress vs. strain curves obtained in different conditions of temperature and strain rates are plotted in Fig. 8. the curves show a net increase in stress with strain up to a peak, at the lower strain rate investigated the peak was followed by a strong flow softening in all the temperatures conditions.

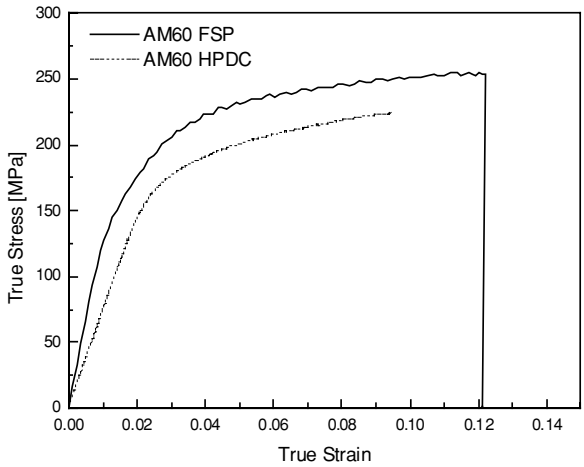

Figure 5 Room temperature tensile behaviour of the as-received material compared with the FSP one.

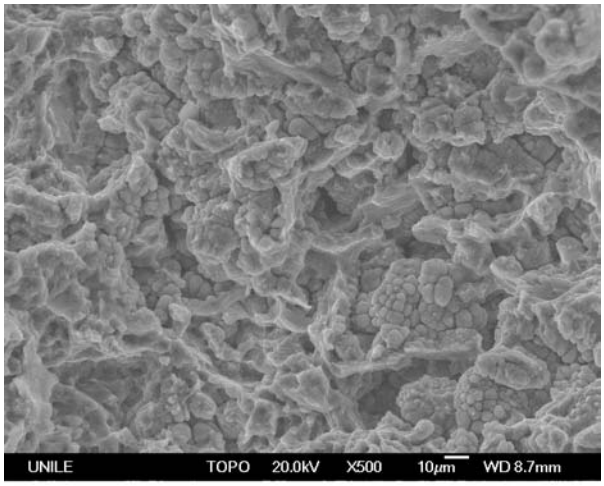

(a)

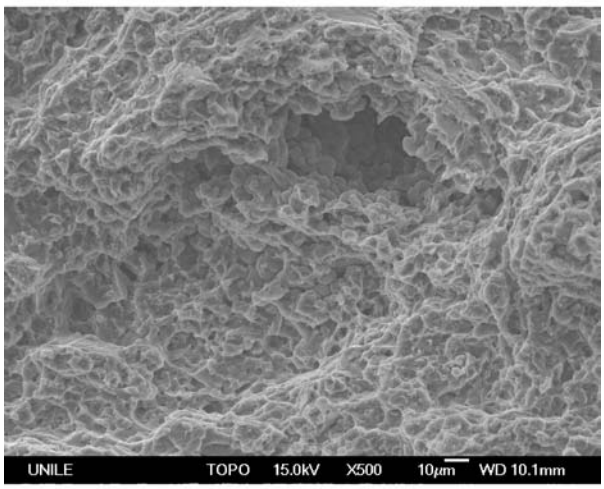

(b)

Figure 6 Fracture surfaces of the HPDC AM60B alloy revealing the big defects.

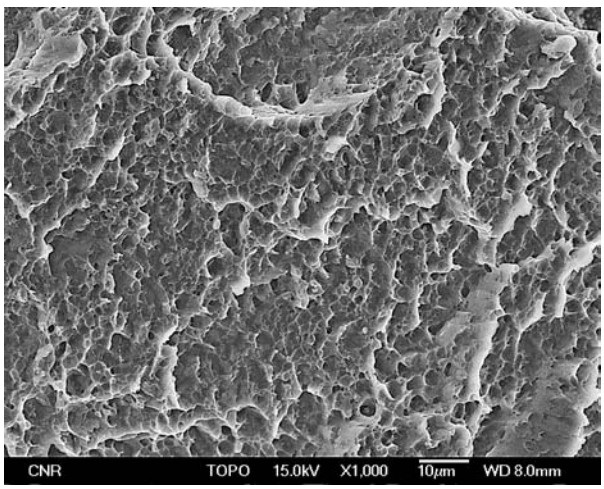

Figure 7 Fracture surface of the FSP AM60B alloy revealing the disappearance of the casting defects.

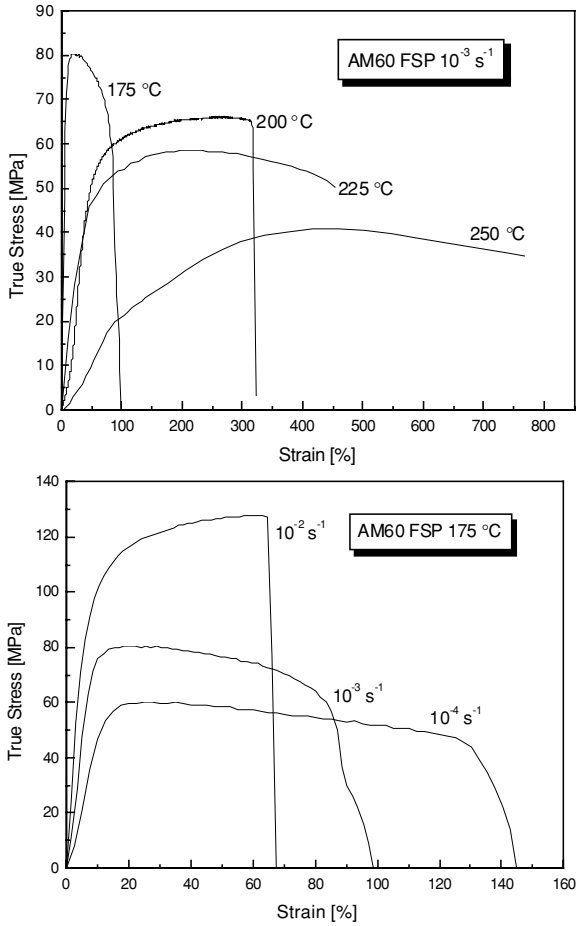

Figure 8 Flow stress vs. strain behaviour of the FSP material at different temperatures and strain rates.

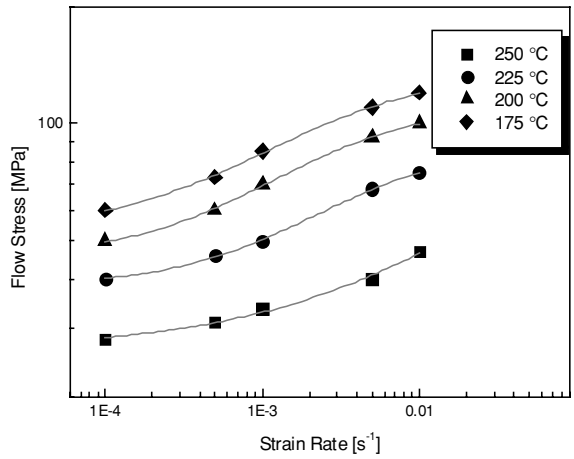

Figure 9 Flow stress vs. strain rate behaviour of the FSP material plotted for all the temperatures investigated.

The Fig. 9 summarizes the flow stress behaviour of the material as a function of strain rate at all the testing temperatures of the present study in a form of double logarithmic plot, the value used in the plot is relative to a true strain of 1.

A superplastic typical sigmoidal behaviour of the flow stress with the initial strain rate for all the investigated

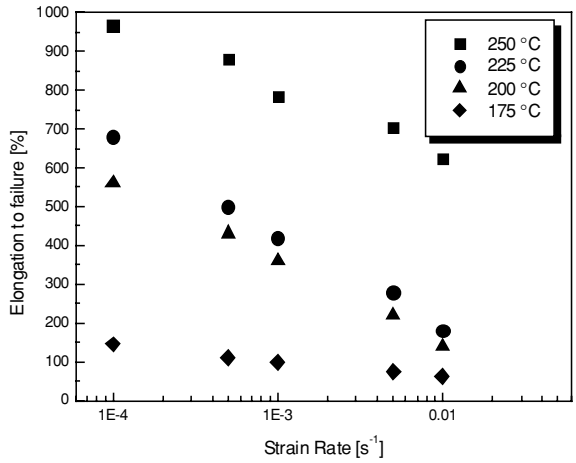

Figure 10 Elongation to fracture vs. strain rate behaviour of the FSP material plotted for all the temperatures investigated.

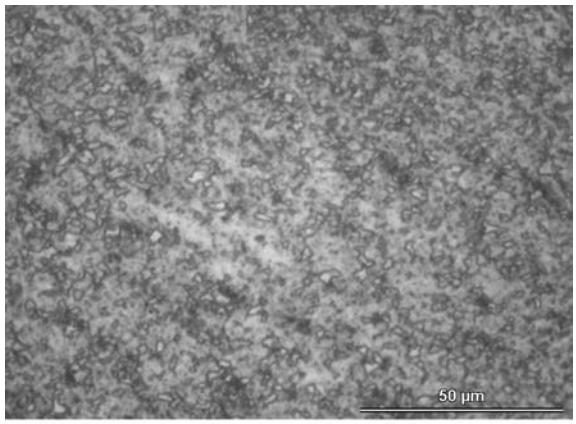

(a)

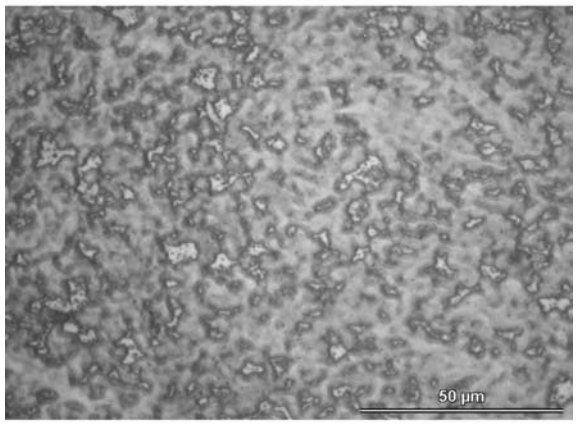

(b)

Figure 11 Optical microstructure of the tensile tested material at 175°C 4 × 10^{-3} s^{-1} (a) and 200°C 4 × 10^{-3} s^{-1} (b).

temperature identifying three different regions of superplastic deformation was recognized, an increase in flow stress as increasing strain rate and decreasing temperature was observed for all the studied conditions.

The variation of the total elongation to failure as a function of the different initial strain rate is shown in Fig. 10, the tensile ductility decrease as increasing the

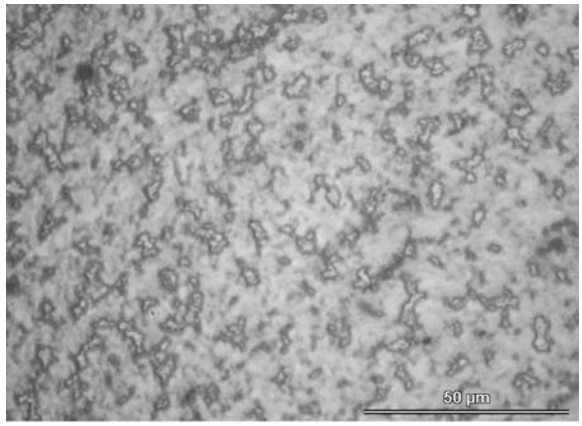

(a)

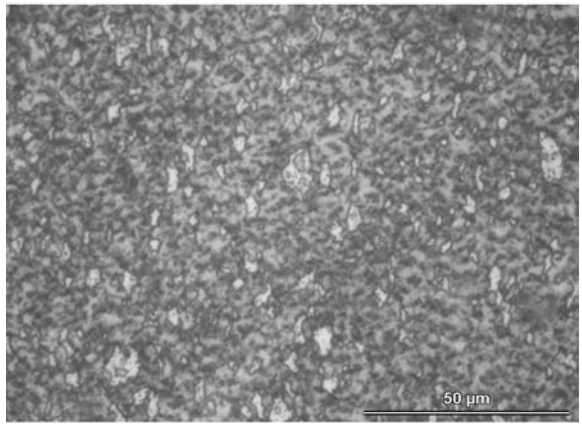

(b)

Figure 12 Optical microstructure of the tensile tested material at 175°C 4 × 10^{-4} s^{-1} (a) and 200°C 4 × 10^{-4} s^{-1} (b).

strain rate for all the temperatures investigated reaching good levels of deformation in the high strain rate regime for the higher temperatures investigated, the fine and stable grain structure leads to the exhibition of exceptional ductility respect to the base material in FSP conditions. From a microstructural point of view, the hot tensile tested material exhibited high temperature recrystallization with the presence of very fine equiaxed grains appearing at 175°C (Fig. 11a). By increasing the testing temperature such grains become larger (Fig. 11b); by decreasing the strain rate, the recrystallized grains appear larger and elongated in the loading direction (Fig. 12) as a consequence of the higher deformation exhibited.

4. Conclusions

The effect of FSP on the mechanical and microstructural behaviour of HPDC AM60B Magnesium alloy was studied and the results are presented in the paper. The material exhibited an increase in room temperature strength and ductility due to the strong grain refinement consequent to the dynamic recrystallization process acting during deformation. The tensile tests performed in the temperature range 175–250°C at different strain rates

showed the occurrence of high ductility levels at testing strain rates above all the strain rates investigated.

References

1. T. G. LANGDON, *Mater. Trans.* **40** (1999) 716.
2. B. L. MORDIKE and T. EBERT, *Mater. Sci. Eng. A* **302** (2001) 37.
3. K. MÁTHIS, Z. TROJANOVÁ, P. LUKÁC, C. H. CÁCERES and J. LENDVAI, *J. All. Com.* **378** (2004) 176.
4. A. RUDAJEVOVA, M. STANEK and P. LUKÁC, *Mater. Sci. Eng. A* **341** (2003) 152.
5. H. WETANABE, T. MUKAI, M. KOHZU, S. TANABE and K. HIGASHI, *Mater. Trans.* **40** (1999) 809.
6. M. MABUKI, K. AMEYAMA, H. IWASAKI and K. HIGASHI, *Acta Mater.* **47** (1999) 2047.
7. A. BUSSIBA, A. BEN ARTZY, A. SHTECHMAN, S. IFERGAN and *M. Kupiec*, *Mater. Sci. Eng. A* **302** (2001) 56.
8. I. CHARIT and R. S. MISHRA, *Mater. Sci. Eng. A.* **359** (2003) 290.
9. Z. Y. MA, R. S. MISHRA and M. W. MAHONEY, *Scripta Mater.* **50** (2004) 931.
10. M. GUERRA, C. SCHMIDT, J. C. MCCLURE, L. E. MURR and A. C. NUNES, *Mater. Charac.* **49** (2003) 95.
11. P. ULYSSE, *Inter. J. Mach. Tools & Manufac.* **42** (2002) 1549.
12. C. G. RHODES, M. W. MAHONEY and W. H. BINGEL, *Scripta Mater.* **36** (1997) 69.
13. H. G. SALEM, A. P. REYNOLDS and J. S. LYONS, *Scripta Mater.* **46** (2002) 337.
14. C. G. RHODES, M. W. MAHONEY, W.H. BINGEL and M. CALABRESE, *ibid.* **48** (2003) 1451.
15. Y. S. SATO, M. URATA, H. KOKAWA and K. IKEDA, *Mater. Sci. Eng. A.* **354** (2003) 298.
16. Y. S. SATO, S. H. C. PARK, A. MATSUNAGA, A. HONDA and H. KOKAWA, *Journal of Mater. Sci.* **40** (3) (2005), 637.

Received 14 March
and accepted 18 July 2005